
ADDRESSING VARIANCE SHRINKAGE IN VARIATIONAL AUTOENCODERS USING QUANTILE REGRESSION

Haleh Akrami

Signal and Image Processing Institute,
Ming Hsieh Department of Electrical and Computer Engineering,
University of Southern California,
Los Angeles, CA, USA
email: akrami@usc.edu

Anand A. Joshi

Signal and Image Processing Institute,
Ming Hsieh Department of Electrical and Computer Engineering,
University of Southern California,
Los Angeles, CA, USA
email: ajoshi@usc.edu

Sergul Aydore

Amazon Web Services,
New York, NY, USA
email: sergulaydore@gmail.com

Richard M. Leahy

Signal and Image Processing Institute,
Ming Hsieh Department of Electrical and Computer Engineering,
University of Southern California,
Los Angeles, CA, USA
email: leahy@sipi.usc.edu

October 20, 2020

ABSTRACT

Estimation of uncertainty in deep learning models is of vital importance, especially in medical imaging, where reliance on inference without taking into account uncertainty could lead to misdiagnosis. Recently, the probabilistic Variational AutoEncoder (VAE) has become a popular model for anomaly detection in applications such as lesion detection in medical images. The VAE is a generative graphical model that is used to learn the data distribution from samples and then generate new samples from this distribution. By training on normal samples, the VAE can be used to detect inputs that deviate from this learned distribution. The VAE models the output as a conditionally independent Gaussian characterized by means and variances for each output dimension. VAEs can therefore use reconstruction probability instead of reconstruction error for anomaly detection. Unfortunately, joint optimization of both mean and variance in the VAE leads to the well-known problem of shrinkage or underestimation of variance. We describe an alternative approach that avoids this variance shrinkage problem by using quantile regression. Using estimated quantiles to compute mean and variance under the Gaussian assumption, we compute reconstruction probability as a principled approach to outlier or anomaly detection. Results on simulated and Fashion MNIST data demonstrate the effectiveness of our approach. We also show how our approach can be used for principled heterogeneous thresholding for lesion detection in brain images.

1 Introduction

Inference based on deep learning methods that does not take into account uncertainty can lead to over-confident predictions, particularly with limited training data (Reinhold et al., 2020). Quantifying uncertainty is particularly important in critical applications such as clinical diagnosis, where a realistic assessment of uncertainty is essential in determining disease status and appropriate treatment. Here we address the important problem of learning uncertainty in order to perform statistically-informed inference.

Unsupervised learning approaches such as the Variational autoencoder (VAE) (Kingma and Welling, 2013) and its variants (Makhzani et al., 2015) can approximate the underlying distribution of high-dimensional data. VAEs are trained using the variational lower bound of the marginal likelihood of data as the objective function. They can then be used to generate samples from the data distribution, where probabilities at the output are modeled as parametric distributions such as Gaussian or Bernoulli that are conditionally independent across output dimensions (Kingma and Welling, 2013).

VAEs are popular for anomaly detection. Once the distribution of anomaly-free samples is learned, during inference we can compute the reconstruction error between a given image and its reconstruction to identify abnormalities (Aggarwal, 2015). Decisions on the presence of outliers in the image are often based on empirically chosen thresholds. An and Cho (2015) proposed to use reconstruction probability rather than the reconstruction error to detect outliers. This allows a more principled approach to anomaly detection since inference is based on quantitative statistical measures and can include corrections for multiple comparisons.

Predictive uncertainty can be categorized in two types: aleatoric uncertainty as a result of unknown or unmeasured features and epistemic uncertainty which is often referred as model uncertainty, as it is the uncertainty due to model limitations (Skafté et al., 2019). Infinite training data do not reduce the former uncertainty in contrast to the latter. Skafté et al. (2019) summarized different methods to estimate uncertainty including Gaussian processes, uncertainty aware neural networks, Bayesian neural networks, and ensemble methods. Another recent approach makes use of collaborative networks (Zhou et al., 2020). While we focus here on anomaly detection, estimating uncertainty has a wide range of applications including reinforcement learning, active learning, and Bayesian optimization (Szepesvari, 2010; Huang et al., 2010; Frazier, 2018; Ross et al., 2008; Reinhold et al., 2020).

Here, we focus on predicting variance use VAEs. These variances represent an aleatoric uncertainty associated with the conditional variance of the estimates given the data (Reinhold et al., 2020). Estimating the variance is more challenging than estimating the mean in generative networks due to the unbounded likelihood (Skafté et al., 2019). In the case of VAEs, if the conditional mean network prediction is nearly perfect (zero reconstruction error), then maximizing the log-likelihood pushes the estimated variance towards zero in order to maximize likelihood. This also makes VAEs susceptible to overfitting the training data. These near-zero variance estimates, with the log-likelihood approaching an infinite supremum, do not lead to a good generative model. It has been shown that there is a strong link between this likelihood blow-up and the mode-collapse phenomenon (Mattei and Frellsen, 2018; Reinhold et al., 2020). In fact, in this case, the VAE behaves much like a deterministic autoencoder (Blaauw and Bonada, 2016).

VAEs are among the most widely used generative models. However, while the classical formulation of VAEs allows both mean and variance estimates (Kingma and Welling, 2013), because of the variance shrinkage problem, most if not all implementations estimate only the mean with the variance assumed constant (Skafté et al., 2019).

Here we describe an approach that overcomes the variance shrinkage problem in VAEs using quantile regression (QR) in place of variance estimation. We then demonstrate this new QR-VAE by computing reconstruction probabilities for an anomaly detection task.

Related Work: A few recent papers have targeted the variance shrinkage problem. Among these, Detlefsen et al. (2019) describe reliable estimation of the variance using Comb-VAE, a locally aware mini-batching framework that includes a scheme for unbiased weight updates for the variance network. In an alternative approach, Stirn and Knowles (2020) suggest treating variance variationally, assuming a Student’s t likelihood for the posterior to prevent optimization instabilities and assume a Gamma prior for the precision parameter of this distribution. The resulting Kullback–Leibler (KL) divergence induces gradients that prevent the variance from approaching zero (Stirn and Knowles, 2020).

Our Contribution: To address the variance shrinkage problem, we suggest an alternative and attractively simple solution: assuming the output of the VAE has a Gaussian distribution, we quantify uncertainty in VAE estimates using conditional quantile regression (QR-VAE). The aim of conditional quantile regression (Koenker and Bassett Jr, 1978) is to estimate a quantile of interest. Here we use these quantiles to compute variance, thus sidestepping the shrinkage problem. It has been shown that quantile regression is able to capture aleatoric uncertainty (Tagasovska and Lopez-Paz, 2019). We demonstrate the effectiveness of our method quantitatively and qualitatively on simulated and real-world datasets. Our approach is computationally efficient and does not add any complication to training or sampling procedures.

2 Background

Before introducing our approach, we first define mathematical notations and briefly explain the VAE formulation and the variance shrinkage problem. We also summarize the conditional quantile regression formulation.

2.1 Variance Shrinkage Problem in Variational Autoencoders

Let $x_i \in \mathbb{R}^D$ be an observed sample of random variable X where $i \in \{1, \dots, N\}$, D is the number of features and N is the number of samples; and let z_i be an observed sample for latent variable Z where $j \in \{1, \dots, S\}$. Given a sample x_i representing an input data, VAE is a probabilistic graphical model that estimates the posterior distribution $p_\theta(Z|X)$ as well as the model evidence $p_\theta(X)$, where θ are the generative model parameters (Kingma and Welling, 2013). The VAE approximates the posterior distribution of Z given X by a tractable parametric distribution and minimizes the ELBO loss (An and Cho, 2015). It consists of the encoder network that computes $q_\phi(Z|X)$, and the decoder network that computes $p_\theta(X|Z)$ (Wingate and Weber, 2013), where ϕ and θ are model parameters. The marginal likelihood of an individual data point can be rewritten as follows:

$$\log p_\theta(x_i) = D_{KL}(q_\phi(Z|x_i), p_\theta(Z|x_i)) + L(\theta, \phi; x_i), \quad (1)$$

where

$$L(\theta, \phi; x_i) = \mathbb{E}_{q_\phi(Z|x_i)}[\log(p_\theta(x_i|Z))] - D_{KL}(q_\phi(Z|x_i)||p_\theta(Z)). \quad (2)$$

The first term (log-likelihood) in equation 2 can be interpreted as the *reconstruction loss* and the second term (KL divergence) as the *regularizer*. The total loss over all samples can be written as:

$$L(\theta, \phi, X) = L_{REC} + L_{KL} \quad (3)$$

where $L_{REC} := \mathbb{E}_{q_\phi(Z|X)}[\log(p_\theta(X|Z))]$ and $L_{KL} := D_{KL}(q_\phi(Z|X)||p_\theta(Z))$.

Assuming the posterior distribution is Gaussian and using 1-sample approximation (Skafta et al., 2019), the likelihood term simplifies to:

$$L_{REC} = \sum_i \frac{-1}{2} \log(\sigma_\theta^2(x_i)) - \frac{(x_i - \mu_\theta(z_i))^2}{2\sigma_\theta^2(z_i)} \quad (4)$$

where $p(Z) = \mathcal{N}(0, I)$, $p_\theta(X|Z) = \mathcal{N}(X|\mu_\theta(Z), \sigma_\theta(Z))$, and $q_\phi(Z|X) = \mathcal{N}(Z|\mu_\phi(X), \sigma_\phi(X))$.

Optimizing VAEs with a Gaussian posterior is difficult (Skafta et al., 2019). If the model has sufficient capacity that there exists (ϕ, θ) for which $\mu_\theta(z)$ provides a sufficiently good reconstruction, then the second term pushes the variance to zero before the term $\frac{-1}{2} \log(\sigma_\theta^2(x_i))$ catches up (Blaauw and Bonada, 2016; Skafta et al., 2019).

One good example of this behavior is in speech processing applications (Blaauw and Bonada, 2016). The input is a spectral envelope which is a relatively smooth 1D curve. Representing this as a 2D image produces highly structured and simple training images. As a result, the model quickly learns how to accurately reconstruct the input. Consequently, reconstruction errors are small and the estimated variance becomes vanishingly small. Another example is 2D reconstruction of MRI images where the images from neighbouring 2D slices are highly correlated leading again to variance shrinkage (Volokitin et al., 2020). To overcome this problem, variance estimation networks are avoided by using a Bernoulli distribution or the variance is simply set to a constant value (Skafta et al., 2019).

2.2 Conditional Quantile Regression

In contrast to classical parameter estimation where the goal is to estimate the conditional mean of the response variable given the feature variable, the goal of quantile regression is to estimate conditional quantiles based on the data (Yu and Moyeed, 2001; Koenker and Hallock, 2001). The most common application of quantile regression models is in the cases in which parametric likelihood cannot be specified (Yu and Moyeed, 2001).

Quantile regression can be used to estimate the conditional median (0.5 quantile) or other quantiles of the response variable conditioned on the feature variable. The α -th conditional quantile function is defined as $q_\alpha(x) := \inf\{y \in \mathbb{R} : F(y|X = x) \geq \alpha\}$ where $F = P(Y \leq y)$ is strictly monotonic cumulative distribution function. Similar to classical

regression analysis which estimates the conditional mean, the α -th quantile regression ($0 < \alpha < 1$) seeks a solution to the following minimization problem for input x and output y (Koenker and Bassett Jr, 1978; Yu and Moyeed, 2001):

$$\arg \min_{\theta} \sum_i \rho_{\alpha}(y_i - f_{\theta}(x_i)) \tag{5}$$

where x_i are the inputs, y_i are the responses, ρ_{α} is the *check function* or *pinball loss* (Koenker and Bassett Jr, 1978) and f is the model parameterized by θ . The goal is to estimate the parameter θ of the model f . The *pinball loss* is defined as:

$$\rho_{\alpha}(y, \hat{y}) := \begin{cases} \alpha(y - \hat{y}) & \text{if } (y - \hat{y}) > 0 \\ (1 - \alpha)(y - \hat{y}) & \text{otherwise.} \end{cases} \tag{6}$$

Due to its simplicity and generality, quantile regression is widely applicable in classical regression and machine learning to obtain a conditional prediction interval (Rodrigues and Pereira, 2020). It can be shown that minimization of the loss function in equation 5 is equivalent to maximization of the likelihood function formed by combining independently distributed asymmetric Laplace densities (Yu and Moyeed, 2001):

$$\arg \max_{\theta} L(\theta) = \frac{\alpha(1 - \alpha)}{\sigma} \exp \left\{ \frac{-\sum_i \rho_{\alpha}(y_i - f_{\theta}(x_i))}{\sigma} \right\}$$

where σ is the scale parameter.

3 Proposed Approach: Uncertainty Estimation for Autoencoders with Quantile Regression (QR-VAE)

Instead of estimating the conditional mean and conditional variance directly at each pixel (or feature), the outputs of our QR-VAE are multiple quantiles of the output distributions at each pixel. This is done by replacing the Gaussian likelihood term in the VAE loss function with the quantile loss (check or pinball loss). For the QR-VAE, if we assume a Gaussian output, then only two quantiles are needed to fully characterize the Gaussian distribution. Specifically, we estimate the median and 0.15-th quantile, which corresponds to one standard deviation from the mean. Our QR-VAE outputs, Q_L (low quantile) and Q_H (high quantile), are then used to calculate the mean and the variance. To find these conditional quantiles, fitting is achieved by minimization of the pinball loss for each quantile. The resulting reconstruction loss for the proposed model can be calculated as:

$$L_{REC} = \sum_i \rho_L(x_i - f_{\theta_L}(x_i)) + \sum_i \rho_H(x_i - f_{\theta_H}(x_i))$$

where θ_L and θ_H are the parameters of the models corresponding to the quantiles Q_L and Q_H , respectively. These quantiles are estimated for each output pixel or dimension.

We prevent quantile crossing (He, 1997) by limiting the flexibility of independent quantile regression since both quantiles are estimated simultaneously rather than training separate networks for each quantile (Rodrigues and Pereira, 2020). Note that the estimated quantiles share the network parameters except for the last layer.

4 Experiments and results

We evaluate our proposed approach on (i) A simulated dataset for density estimation; (ii) Variance estimation in the Fashion-MNIST dataset; and (iii) Lesion detection in a brain imaging dataset. We compare our results qualitatively and quantitatively, using KL divergence between the learned distribution and the original distribution, for the simulated data with Comb-VAE (Skafte et al., 2019) and VAE as baselines. We compare our lesion detection results with the VAE which estimates both the mean and the variance. The Area under the receiver operating characteristic curve (AUC) is used as a performance metric. We performed the lesion detection task by directly estimating a 95% confidence interval.

4.1 Simulations

Following Skafte et al. (2019), we first evaluate our variance estimation using VAE, Comb-VAE, and QR-VAE on a simulated dataset. The two moon dataset inspires the data generation process for this dataset¹. First, we generate 500

¹https://scikit-learn.org/stable/modules/generated/sklearn.datasets.make_moons

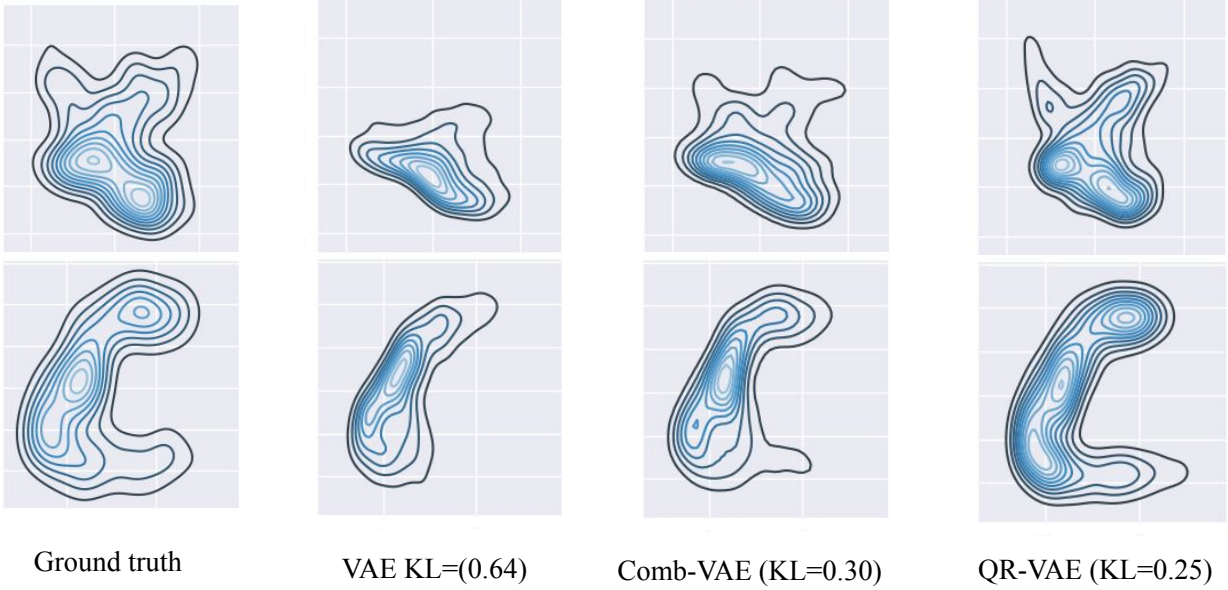


Figure 1: Pairwise joint distribution of the ground truth and distributions. Top: v_1 vs. v_2 dimensions. Bottom: v_2 vs v_3 dimensions. From left to right: original distribution and distributions computed using VAE, Comb-VAE and QR-VAE, respectively. We also show the KL divergence between the learned distribution and the original distribution.

points in \mathbb{R}^2 in a two-moon manner to generate a known two-dimensional latent space. These are then mapped to four dimensions (v_1, v_2, v_3, v_4) by using the following equations:

$$\begin{aligned}
 v_1(z_1, z_2) &= z_1 - z_2 + \epsilon \sqrt{0.03 + 0.05(3 + z_1)} \\
 v_2(z_1, z_2) &= z_1^2 - \frac{1}{2}z_2 + \epsilon \sqrt{0.03 + 0.03\|z_1\|_2} \\
 v_3(z_1, z_2) &= z_1z_2 - z_1 + \epsilon \sqrt{0.03 + 0.05\|z_1\|_2} \\
 v_4(z_1, z_2) &= z_1 + z_2 + \epsilon \sqrt{0.03 + \frac{0.03}{0.02 + \|z_1\|_2}}
 \end{aligned}$$

where ϵ is sampled from a normal distribution. For more details about the simulation, please refer to Skafte et al. (2019)². After training the models, we first sample from z and then from the posteriors using the estimated means and variances from the decoder. The distribution of these generated samples represents the learned distribution in the generative model.

In Figure 1, we plot pairwise joint distribution for the input data as well as the generated samples using various models. We used Gaussian kernel density estimation (Parzen, 1962) for modeling the distributions from 1000 samples in each case. We observe that the standard VAE underestimates the variance resulting in insufficient learning of the data distribution. The samples from our QR-VAE model capture a data distribution more similar to the ground truth than either standard VAE or Comb-VAE. Our model also outperforms VAE and Comb-VAE in terms of KL divergence between input samples and generated samples as can be seen in Figure 1. The KL divergence is calculated using universal-divergence, which estimates the KL divergence based on k-nearest-neighbor (k-NN) distance (Wang et al., 2009)³.

²https://github.com/SkafteNicki/john/blob/master/toy_vae.py

³<https://pypi.org/project/universal-divergence>

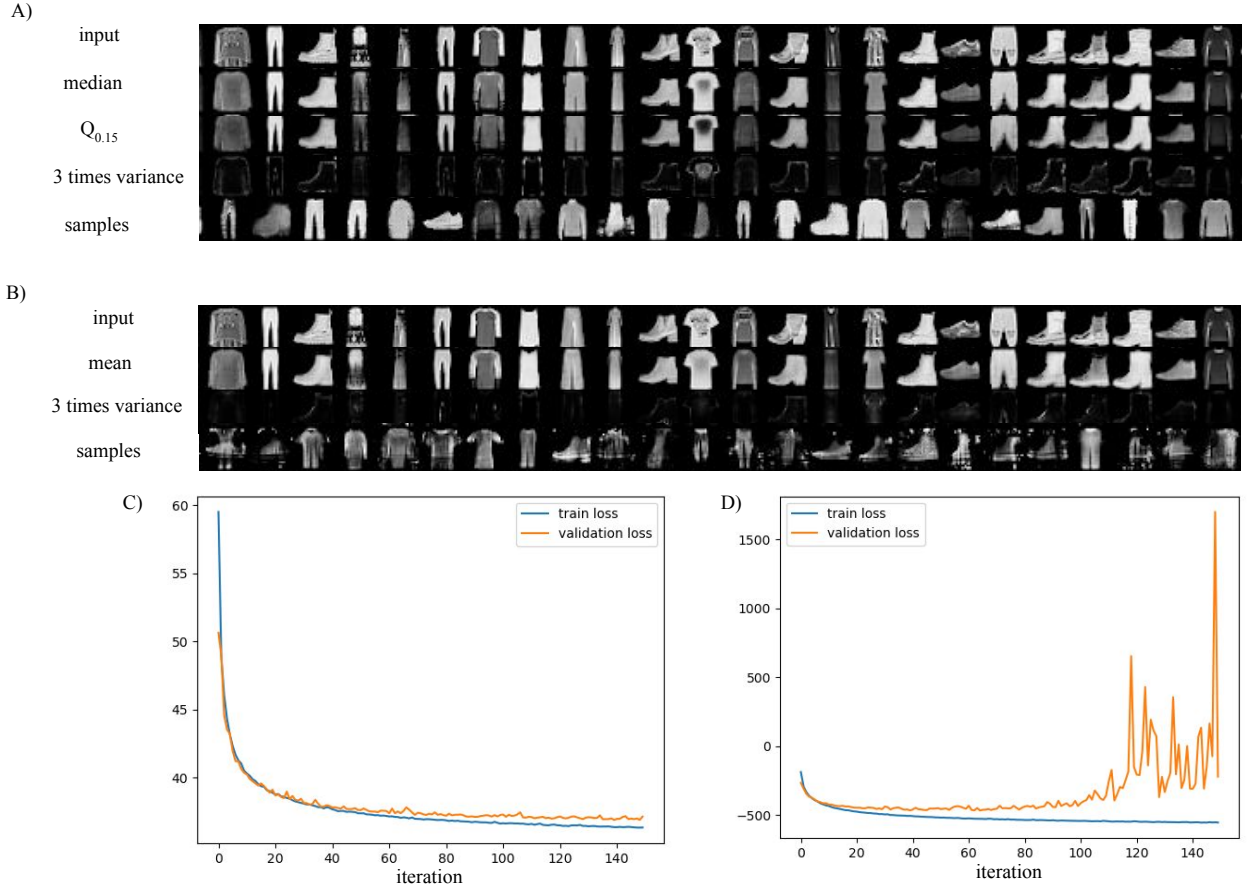


Figure 2: Estimating the variance in Fashion-MNIST dataset using A) QR-VAE where median ($Q_{0.5}$) and $Q_{0.15}$ quantiles are estimated. B) VAE where mean and variance are estimated. Training and validation loss curves for C) QR-VAE D) VAE.

4.2 Estimating Variance in Fashion-MNIST

In the second experiment, we trained VAE and QR-VAE on the Fashion-MNIST dataset (Xiao et al., 2017) where the outputs are: (i) mean and variance, and (ii) 0.15, 0.5 quantiles, respectively. The Fashion-MNIST dataset consists of 70,000 28x28 grayscale images of fashion products from 10 categories (7,000 images per category).

The VAE and QR-VAE models for Fashion-MNIST experiments have the same architecture, except for the last layer. We use fully-connected layers with a single hidden layer consisting of 400 units both for the encoder and decoder. Figure 2 shows the estimated variance along with the estimated mean for VAE and estimated quantiles for QR-VAE. We also show randomly generated samples for both models. It can be seen that the estimated variance using QR-VAE is structured and interpretable as it predicts a high variance around an object’s boundaries. The estimated variance using VAE is much lower than QR-VAE due to variance shrinkage. Moreover, instability in optimization of the VAE loss results in a diverging validation loss curve (Figure 2(D)), which indicates overfitting. The validation loss of QR-VAE is much better (Figure 2(E)). Furthermore, variance shrinkage in VAE produces severely deteriorated sample quality due to mode collapse (Figure 2(D)), which is not the case for QR-VAE (Figure 2(C)).

4.3 Unsupervised Lesion Detection

Finally, we demonstrate utility of the proposed QR-VAE for a medical imaging application of detecting brain lesions. Multiple automatic lesion detection approaches have been developed to assist clinicians in identifying and delineating lesions caused by congenital malformations, tumors, stroke or brain injury. The VAE is a popular framework among the class of unsupervised methods (Chen and Konukoglu, 2018; Baur et al., 2018; Pawlowski et al., 2018). After training a VAE on a lesion free dataset, presentation of a lesioned brain to the VAE will typically result in reconstruction of a

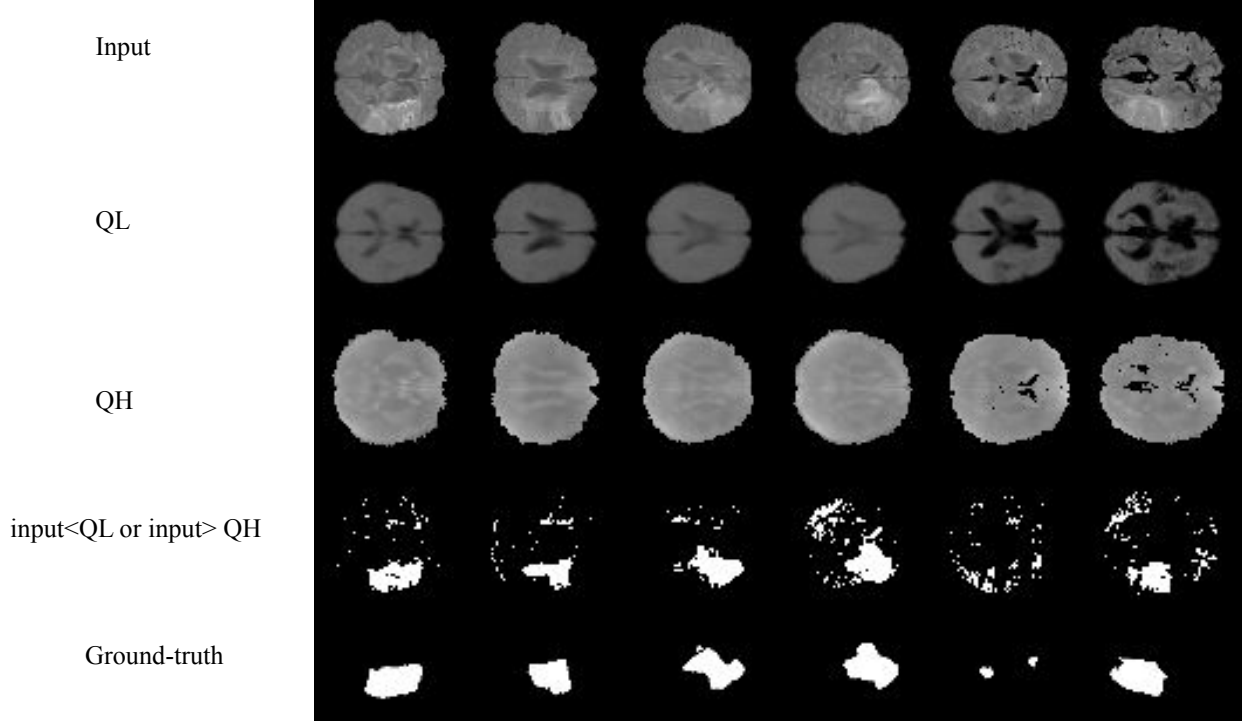


Figure 3: Lesion detection for ISLES dataset using $Q_L = Q_{0.025}$ and $Q_H = Q_{0.975}$. For lesion detection, we consider the pixels outside the $[Q_L, Q_H]$ interval as outliers. Estimated quantiles are the outputs of QR-VAE.

lesion-free equivalent. The error between input and output images can therefore be used to detect and localize lesions. However, selecting an appropriate threshold that differentiates lesion from noise is a difficult task. Furthermore, using a single global threshold across the entire image will inevitably lead to a poor trade-off between true and false positive rates. Using the QR-VAE, we can compute the conditional mean and variance of each output pixel. This allows a more reliable and statistically principled approach for detecting anomalies by thresholding based on computed p-values.

The network architectures of VAE, QR-VAE are chosen based on the previously established architectures (Larsen et al., 2015). Both the VAE and QR-VAE consist of three consecutive blocks of convolutional layer, a batch normalization layer, a rectified linear unit (ReLU) activation function and a fully-connected layer in the bottleneck for the encoder. The decoder includes three consecutive blocks of deconvolutional layers, a batch normalization layer and ReLU followed by the output layer that has 2 separate deconvolution layers (for each output) with Sigmoid activations. For the VAE, the outputs represent mean and variance while for QR-VAE the outputs represent two quantiles from which the conditional mean and variance are computed at each voxel. The size of the input layer is $3 \times 64 \times 64$ where the first dimension represents three different MRI contrasts: T1-weighted, T2-weighted, and FLAIR for each image.

For the training, we use 20 central axial slices of brain MRI datasets from a combination of 119 subjects from the Maryland MagNeTS study (Gullapalli, 2011) of neurotrauma and 112 subjects from the TrackTBI-Pilot (Yue et al., 2013) dataset, both available for download from <https://fitbir.nih.gov>. We use 2D slices rather than 3D images to make sure we had a large enough dataset for training the VAE. These datasets contain T1, T2, and FLAIR images for each subject, and have sparse lesions. We have found that in practice both VAEs have some robustness to lesions in these training data so that they are sufficient for the network to learn to reconstruct lesion-free images as required for our anomaly detection task. The three imaging modalities (T1, T2, FLAIR) were rigidly co-registered within subject and to the MNI brain atlas reference and re-sampled to 1mm isotropic resolution. Skull and other non-brain tissue were removed using BrainSuite (<https://brainsuite.org>). Subsequently, we reshaped each sample into 64×64 dimensional images and performed histogram equalization to a lesion free reference. We evaluated the performance of our model on a test set consisting of 20 central axial slices of 15 subjects from the ISLES (The Ischemic Stroke Lesion Segmentation) database (Maier et al., 2017) for which ground truth, in the form of manually-segmented lesions, is also provided. We performed similar pre-processing as for the training set.

For simplicity, we first performed the lesion detection task using the QR-VAE without the Gaussian assumption as shown in Figure 3. We trained the QR-VAE to estimate the $Q_{0.025}$ and $Q_{0.975}$ quantiles. We then used these quantiles

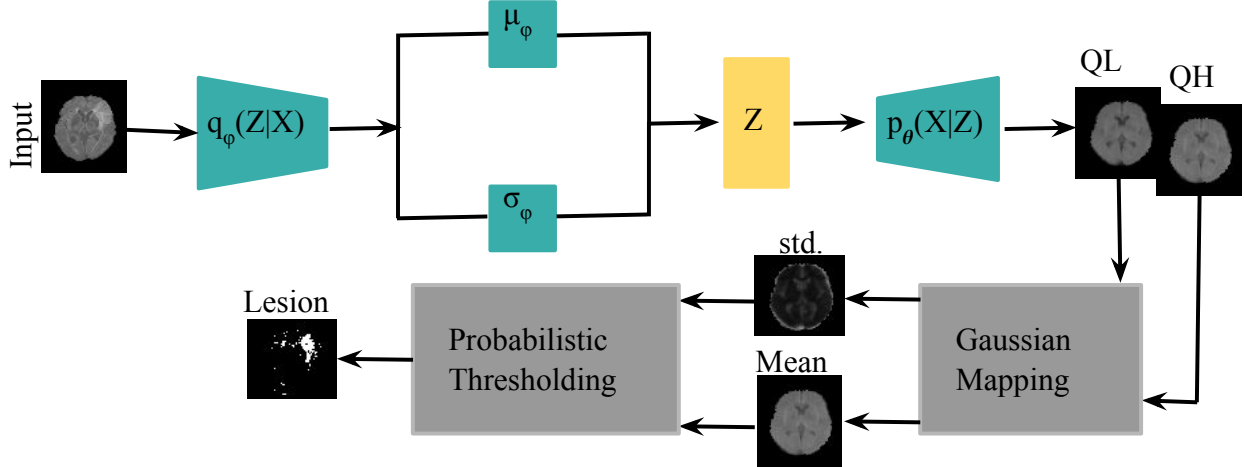


Figure 4: Estimating two quantiles in ISLES dataset using QR-VAE. Using the Gaussian assumption for the posterior, there is 1-1 mapping from these quantiles to mean and standard deviation.

directly to threshold the input images for anomalies. This leads to a 5% false positive rate. This method is simple and avoids the need for validation data to determine an appropriate threshold. However, without access to p-values we are unable to determine a threshold that can be used to correct for multiple comparisons by controlling the false-discovery or family-wise error rate.

In a second experiment, we trained a VAE with a Gaussian posterior and the QR-VAE as summarized in Figure 4, in both cases estimating conditional mean and variance. Specifically, we estimated the $Q_{0.15}$ and $Q_{0.5}$ quantiles for the QR-VAE and mapped these values to pixel-wise mean and variance. We then used these means and variances to convert image intensities to p-values. Since we are applying the threshold separately at each pixel, there is the potential for a large number of false positives simply because of the number of tests performed. For example, thresholding at an $\alpha = 0.05$ significance level could result in up to 5% of the pixels being detected as anomalies. In practice the false positive rate is likely to be lower because of spatial correlations between pixels. To avoid an excessive number of false positives we threshold based on corrected p-values calculated to control the False Discovery Rate (FDR), that is the fraction of detected anomalies that are false positives (Benjamini and Hochberg, 1995). We chose the thresholds corresponding to an FDR corrected p-value of 0.05. As shown in Figure 5, the VAE underestimates the variance, so that most of the brain shows significant p-values, even with FDR correction. On the other hand, the QR-VAE’s thresholded results detect anomalies that reasonably match the ground truth. To produce a quantitative measure of performance, we also computed the area under the ROC curve (AUC) for VAE and QR-VAE. To do this we first computed z-score images by subtracting the mean and normalizing by standard deviation. We then applied a median filtering with a 7×7 window. By varying the threshold on the resulting images and comparing it to ground truth, we obtained AUC values of 0.56 for the VAE and 0.94 for the QR-VAE.

5 Conclusion

Simultaneous estimation of the mean and the variance in VAE underestimates the true variance leading to instabilities in optimization (Skafte et al., 2019). For this reason, classical VAE formulations that include both mean and variance estimates are rarely used in practice. Typically, only the mean is estimated with variance assumed constant (Skafte et al., 2019). To address this problem in variance estimation, we propose an alternative quantile-regression model (QR-VAE) for improving the quality of variance estimation. We use quantile regression and leverage the Gaussian assumption to obtain the mean and variance by estimating two quantiles. We show that our approach outperforms VAE as well as a Comb-VAE which is an alternative approach for addressing the same issue, in a synthetic dataset, the Fashion-MNIST dataset, and brain imaging datasets. Our approach also has more straightforward implementation compared to Comb-VAE. As a demonstrative application, we use our QR-VAE model to obtain a probabilistic heterogeneous threshold for a brain lesion detection task. This threshold results in a completely unsupervised lesion (or anomaly) detection method that avoids the need for a labeled validation dataset for principled selection of an appropriate threshold to control the false discovery rate.

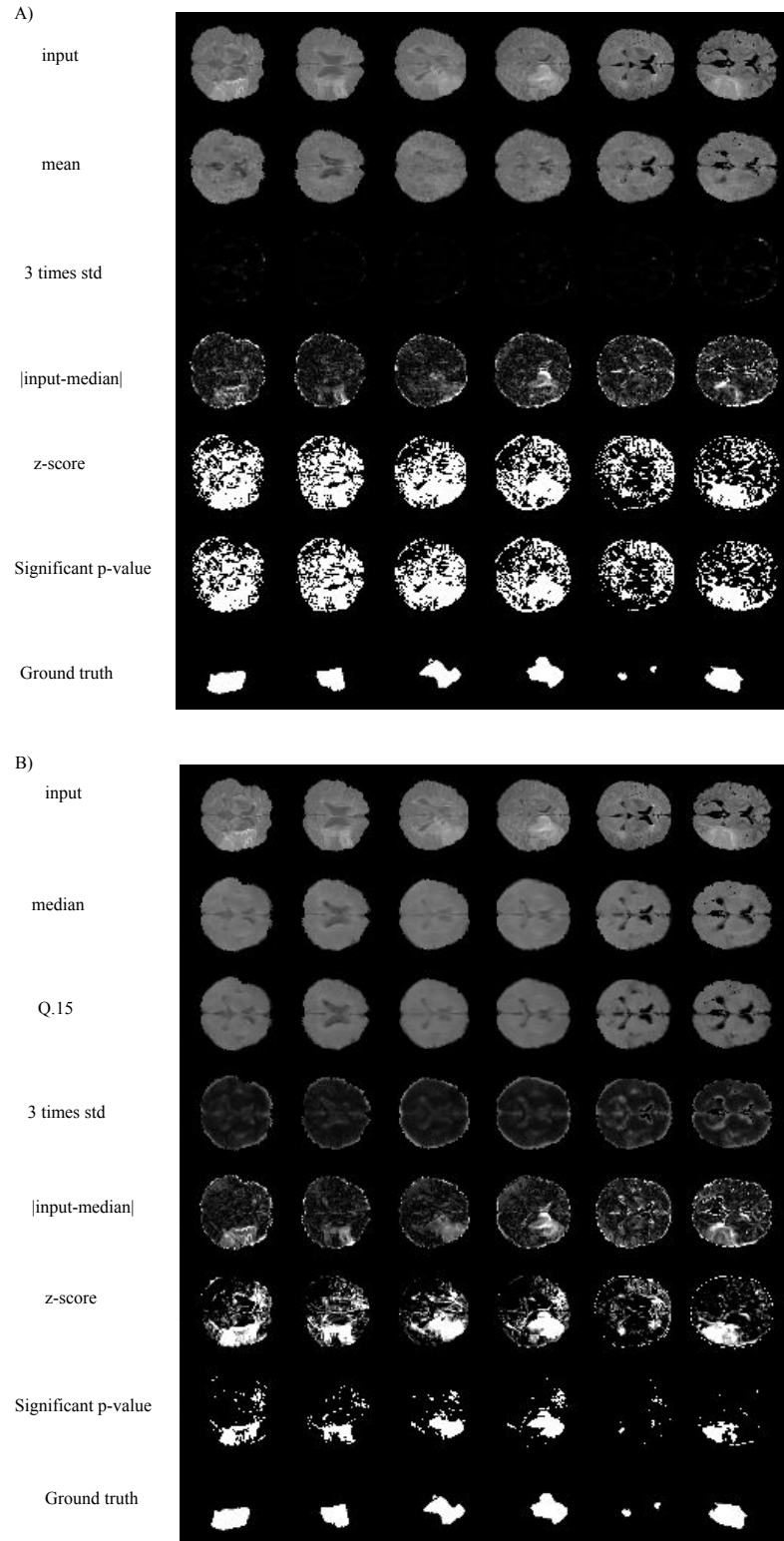


Figure 5: Lesion detection for the ISLES dataset. A) VAE with mean and variance estimation B) QR-VAE. First, we normalize each pixel value using the pixel-wise model’s estimates of mean and variance. The resulting z score is then converted to an FDR-corrected p-value and the images are thresholded at a significance level of 0.05. The bottom rows are ground truth based on expert manual segmentation of lesions.

Acknowledgements

This work is supported by the following grants: R01 NS074980, W81XWH-18-1-0614, R01 NS089212, and R01 EB026299.

References

- Aggarwal, C. C. (2015). Outlier analysis. In *Data mining*, pages 237–263. Springer.
- An, J. and Cho, S. (2015). Variational autoencoder based anomaly detection using reconstruction probability. *Special Lecture on IE*, 2(1):1–18.
- Baur, C., Wiestler, B., Albarqouni, S., and Navab, N. (2018). Deep autoencoding models for unsupervised anomaly segmentation in brain mr images. In *International MICCAI Brainlesion Workshop*, pages 161–169. Springer.
- Benjamini, Y. and Hochberg, Y. (1995). Controlling the false discovery rate: a practical and powerful approach to multiple testing. *Journal of the Royal statistical society: series B (Methodological)*, 57(1):289–300.
- Blaauw, M. and Bonada, J. (2016). Modeling and transforming speech using variational autoencoders. *Morgan N, editor. Interspeech 2016; 2016 Sep 8-12; San Francisco, CA.[place unknown]: ISCA; 2016. p. 1770-4.*
- Chen, X. and Konukoglu, E. (2018). Unsupervised detection of lesions in brain MRI using constrained adversarial auto-encoders. *arXiv preprint arXiv:1806.04972*.
- Detlefsen, N. S., Jørgensen, M., and Hauberg, S. (2019). Reliable training and estimation of variance networks. *arXiv preprint arXiv:1906.03260*.
- Frazier, P. I. (2018). A tutorial on bayesian optimization. *arXiv preprint arXiv:1807.02811*.
- Gullapalli, R. P. (2011). Investigation of prognostic ability of novel imaging markers for traumatic brain injury (tbi). Technical report, BALTIMORE UNIV MD.
- He, X. (1997). Quantile curves without crossing. *The American Statistician*, 51(2):186–192.
- Huang, S.-J., Jin, R., and Zhou, Z.-H. (2010). Active learning by querying informative and representative examples. In *Advances in neural information processing systems*, pages 892–900.
- Kingma, D. P. and Welling, M. (2013). Auto-encoding variational bayes. *arXiv preprint arXiv:1312.6114*.
- Koenker, R. and Bassett Jr, G. (1978). Regression quantiles. *Econometrica: journal of the Econometric Society*, pages 33–50.
- Koenker, R. and Hallock, K. F. (2001). Quantile regression. *Journal of economic perspectives*, 15(4):143–156.
- Larsen, A. B. L., Sønderby, S. K., Larochelle, H., and Winther, O. (2015). Autoencoding beyond pixels using a learned similarity metric. *arXiv preprint arXiv:1512.09300*.
- Mai, O., Menze, B. H., von der Gabelentz, J., Häni, L., Heinrich, M. P., Liebrand, M., Winzeck, S., Basit, A., Bentley, P., Chen, L., et al. (2017). ISLES 2015-a public evaluation benchmark for ischemic stroke lesion segmentation from multispectral MRI. *Medical image analysis*, 35:250–269.
- Makhzani, A., Shlens, J., Jaitly, N., Goodfellow, I., and Frey, B. (2015). Adversarial autoencoders. *arXiv preprint arXiv:1511.05644*.
- Mattei, P.-A. and Frellsen, J. (2018). Leveraging the exact likelihood of deep latent variable models. In *Advances in Neural Information Processing Systems*, pages 3855–3866.
- Parzen, E. (1962). On estimation of a probability density function and mode. *The annals of mathematical statistics*, 33(3):1065–1076.
- Pawlowski, N., Lee, M. C., Rajchl, M., McDonagh, S., Ferrante, E., Kamnitsas, K., Cooke, S., Stevenson, S., Khetani, A., Newman, T., et al. (2018). Unsupervised lesion detection in brain ct using bayesian convolutional autoencoders. *OpenReview*.
- Reinhold, J. C., He, Y., Han, S., Chen, Y., Gao, D., Lee, J., Prince, J. L., and Carass, A. (2020). Validating uncertainty in medical image translation. *arXiv preprint arXiv:2002.04639*.
- Rodrigues, F. and Pereira, F. C. (2020). Beyond expectation: deep joint mean and quantile regression for spatiotemporal problems. *IEEE Transactions on Neural Networks and Learning Systems*.
- Ross, S., Chaib-draa, B., and Pineau, J. (2008). Bayesian reinforcement learning in continuous pomdps with application to robot navigation. In *2008 IEEE International Conference on Robotics and Automation*, pages 2845–2851. IEEE.

- Skafté, N., Jørgensen, M., and Hauberg, S. (2019). Reliable training and estimation of variance networks. In *Advances in Neural Information Processing Systems*, pages 6323–6333.
- Stirn, A. and Knowles, D. A. (2020). Variational variance: Simple and reliable predictive variance parameterization. *arXiv preprint arXiv:2006.04910*.
- Szepesvari, C. (2010). Algorithms for reinforcement learning: Synthesis lectures on artificial intelligence and machine learning. *Morgan and Claypool*.
- Tagasovska, N. and Lopez-Paz, D. (2019). Single-model uncertainties for deep learning. In *Advances in Neural Information Processing Systems*, pages 6417–6428.
- Volokitin, A., Erdil, E., Karani, N., Tezcan, K. C., Chen, X., Van Gool, L., and Konukoglu, E. (2020). Modelling the distribution of 3d brain mri using a 2d slice vae. In *International Conference on Medical Image Computing and Computer-Assisted Intervention*, pages 657–666. Springer.
- Wang, Q., Kulkarni, S. R., and Verdú, S. (2009). Divergence estimation for multidimensional densities via k -nearest-neighbor distances. *IEEE Transactions on Information Theory*, 55(5):2392–2405.
- Wingate, D. and Weber, T. (2013). Automated variational inference in probabilistic programming. *arXiv preprint arXiv:1301.1299*.
- Xiao, H., Rasul, K., and Vollgraf, R. (2017). Fashion-MNIST: a novel image dataset for benchmarking machine learning algorithms. *arXiv preprint arXiv:1708.07747*.
- Yu, K. and Moyeed, R. A. (2001). Bayesian quantile regression. *Statistics & Probability Letters*, 54(4):437–447.
- Yue, J. K., Vassar, M. J., Lingsma, H. F., Cooper, S. R., Okonkwo, D. O., Valadka, A. B., Gordon, W. A., Maas, A. I., Mukherjee, P., Yuh, E. L., et al. (2013). Transforming research and clinical knowledge in traumatic brain injury pilot: multicenter implementation of the common data elements for traumatic brain injury. *Journal of neurotrauma*, 30(22):1831–1844.
- Zhou, T., Li, Y., Wu, Y., and Carlson, D. (2020). Estimating uncertainty intervals from collaborating networks. *arXiv preprint arXiv:2002.05212*.